New Phytologist

Research

Abrupt and acclimation responses to changing temperature elicit divergent physiological effects in the diatom *Phaeodactylum tricornutum*

Linda Rehder[1,2], Björn Rost[1,2] and Sebastian D. Rokitta[1]

[1]Alfred-Wegener-Institute, Helmholtz-Centre for Polar and Marine Research, Am Handelshafen 12, Bremerhaven 27570, Germany; [2]FB2 Biology/Chemistry, University of Bremen, Leobener Straße, Bremen 28359, Germany

Author for correspondence:
Linda Rehder
Email: linda.rehder@awi.de

Received: *11 January 2023*
Accepted: *14 April 2023*

New Phytologist (2023) **239:** 1005–1013
doi: 10.1111/nph.18982

Key words: homeostasis, hysteresis, *Phaeodactylum tricornutum*, photosynthesis, phytoplankton, respiration, subcellular, sweet spot.

Summary

- Growth rates and other biomass traits of phytoplankton are strongly affected by temperature. We hypothesized that resulting phenotypes originate from deviating temperature sensitivities of underlying physiological processes.
- We used membrane-inlet mass spectrometry to assess photosynthetic and respiratory O_2 and CO_2 fluxes in response to abrupt temperature changes as well as after acclimation periods in the diatom *Phaeodactylum tricornutum*.
- Abrupt temperature changes caused immediate over- or undershoots in most physiological processes, that is, photosynthetic oxygen release (PS_{O_2}), photosynthetic carbon uptake (PS_{CO_2}), and respiratory oxygen release (R_{O_2}). Over acclimation timescales, cells were, however, able to re-adjust their physiology and revert to phenotypic 'sweet spots'.
- Respiratory CO_2 release (R_{CO_2}) was generally inhibited under high temperature and stimulated under low-temperature settings, on abrupt as well as acclimation timescales. Such behavior may help mitochondria to stabilize plastidial ATP : NADPH ratios and thus maximize photosynthetic carbon assimilation.

Introduction

Phytoplankton are unicellular phototrophic organisms that are responsible for *c.* 50% of the global primary production (Field *et al.*, 1998). By assimilating CO_2 into organic matter via the process of photosynthesis, they provide the nutritional basis for the entire aquatic food web (Beardall & Raven, 2004; Finkel *et al.*, 2009) and act as the prime driver of the biogeochemical cycling of carbon, nitrogen, silicate, phosphorus, and multiple trace metals (Falkowski *et al.*, 1998; Riebesell *et al.*, 2007). Among phytoplankton, diatoms are the most successful taxonomic group, accounting for up to 20% of the global carbon fixation (Tréguer *et al.*, 1995; Falkowski *et al.*, 2000), and up to 40% of the marine primary production (Nelson *et al.*, 1995). They often dominate bloom events (Rousseau, 2000) and contribute disproportionally strong to the vertical carbon export (Gao & Campbell, 2014). Because of this role, diatoms such as the model species *Phaeodactylum tricornutum* have been in the center of many eco-physiological studies.

Phytoplankton cells apply a number of physiological subprocesses that drive metabolism, biomass production, and ultimately growth. In the autotrophic part of metabolism, oxygen (O_2) is released as a by-product of water splitting at the 'start' of photosynthesis, and CO_2 is fixed into sugars in the Calvin cycle at the 'end' of photosynthesis. The heterotrophic part of phytoplankton metabolism primarily extracts energy and reductants from these sugar compounds in processes such as glycolysis or mitochondrial respiration (Falkowski & Raven, 2013). During these processes, CO_2 is released as a product of the tricarboxylic acid cycle (TCA), while O_2 is consumed by the respiratory electron transport chain (Taiz & Zeiger, 2006). Growth, biomass production, and aforementioned physiological subprocesses are affected by environmental factors such as temperature, light intensity, nutrient concentrations, and CO_2 availability, all of which are affected by climate change (Doney *et al.*, 2012).

Temperature is believed to be one of the most profound environmental drivers, since it universally controls molecular movement, and thus, affects literally all physiological processes (Brown *et al.*, 2004; Pörtner *et al.*, 2006; Pearle *et al.*, 2010). Phytoplankton from temperate and polar regions already undergo natural temperature variability on timescales of seasons, mixing, and tidal events. Additionally, next to rising mean sea surface temperatures (Cooley *et al.*, 2022), heat-wave events are projected to increase in frequency, intensity, and duration (Meehl & Tebaldi, 2004; Hobday *et al.*, 2016). Warming that occurs below a process-specific optimum temperature, typically increases physiological rates of the according process. The temperature sensitivity is often described by the Q_{10} law, that is, by the degree of stimulation over a 10°C temperature rise (Hegarty, 1973). However, since physiological processes depend on different physical or

(bio)chemical phenomena, such as diffusion rates, membrane permeability, gas solubility, or enzyme kinetics, they likely diverge significantly in their temperature sensitivities (Padfield *et al.*, 2016; Schuback *et al.*, 2017; Barton *et al.*, 2020). Consequently, temperature rises can be expected to cause physiological imbalances, especially between the complex photosynthetic and respiratory subprocesses. This is even more likely when temperature rises occur beyond thermal optima of processes, where any further warming causes severe rate decreases and physiological detriments (Angilletta Jr & Angilletta, 2009). The sensitivity toward temperature stress also depends on the rate of changes and the species' ability to tolerate transient physiological stress until acclimation is achieved.

Most studies on phytoplankton temperature responses have focused on 'bulk' parameters such as growth or biomass production under acclimated conditions (Eppley, 1972; Bissinger *et al.*, 2008; Boyd *et al.*, 2013), but neglected abrupt responses of single physiological subprocesses. It has been observed that respiratory processes generally seem to be more prominently stimulated by temperature rises than photosynthetic processes (Padfield *et al.*, 2016; Barton *et al.*, 2020). Also, natural phytoplankton communities of temperate or Arctic origin were reported to become relatively more heterotrophic under elevated temperatures (Hoppe *et al.*, 2002; Hancke & Glud, 2004). We hypothesize that abrupt temperature changes cause imbalances between physiological subprocesses and are a major threat for balanced growth. Processes that rely primarily on (bio)physical phenomena, such as charge separation and membrane fluidity (i.e. photosynthetic light reaction) are likely to be differently affected by temperature than processes that involve (bio)chemical pathways (e.g. the tricarboxylic acid cycle). Over acclimation timescales, however, we expect cells to partly overcome imbalances by physiological adjustments (i.e. acclimation) and thereby minimize detrimental effects.

To test these hypotheses, we cultivated *Phaeodactylum tricornutum* at to two different temperature scenarios (6°C vs 15°C). In addition to descriptions of 'bulk' cellular parameters (growth rates, elemental quotas, and pigmentation), cells were exposed to abrupt temperature rises (6°C → 15°C) or drops (15°C → 6°C), respectively, and mass-spectrometric *in-vivo* assays of photosynthetic O_2 release (PS_{O_2}), photosynthetic CO_2 uptake (PS_{CO_2}), respiratory CO_2 release (R_{CO_2}), and respiratory O_2 uptake (R_{O_2}) were conducted.

Materials and Methods

Strain and culture conditions

We cultivated the model species *Phaeodactylum tricornutum* Bohlin, which is known to have different morphotypes that are associated to different habitats and divergent evolutionary adaptation potential (Sabir *et al.*, 2018). Pelagic and benthic strains, however, show very few differences in physiological traits (Raven & Beardall, 2022). The here used triradiate morphotype of *P. tricornutum* (CCAP 1052/1A) was grown at 6°C and 15°C in 0.2 µm sterile-filtered North Sea seawater (Salinity 33), enriched with vitamins and trace metals according to f/2 media (Guillard & Ryther, 1962). Nitrate and phosphate were added in concentrations of 100 and 6 µmol l^{-1}, respectively. Irradiance was applied in a light : dark cycle of 16 h : 8 h with a light intensity of 100 µmol photons m^{-2} s^{-1}. Cells were acclimated to experimental conditions for at least 10 generations. For assessments of growth, chlorophyll quotas and physiological assays, cells were grown as semicontinuous dilute batch cultures in aerated 2 l glass bottles (Schott Instruments, Mainz, Germany) under continuous supply of humidified air (pCO_2 of 400 µatm) generated in a gas mixing system (CGM 2000; MCZ Umwelttechnik, Bad Nauheim, Germany). To ensure temperature stability, culture bottles were placed in aquaria, submersed in temperature-controlled water. Due to logistical reasons, for the determination of elemental composition, incubation bottles with pre-adjusted media (pCO_2 of 400 µatm) were placed on roller tables (*c.* 10 rpm), which avoided sedimentation equally well. In both cultivation approaches, culture densities never exceeded *c.* 60 000 cells ml^{-1}, which ensured nutrient replete conditions and stable carbonate chemistry (pH drift ≤ 0.02; Supporting Information Table S1).

Acclimation responses

Specific growth rates were calculated using the daily assessments of cell concentrations over the exponential growth phase according to the formula $\mu = (\log_e(N_1) - \log_e(N_0))/(t_1 - t_0)$, where μ is the specific growth rate (d^{-1}), and N_0 as well as N_1 are the cell concentrations at the initial and final time points t_0 and t_1, respectively. Counting was performed, using a cell-counter (Beckmann-Coulter Multisizer III, Fullerton, CA, USA). Counting and cell harvests for the determination of particulate organic carbon and nitrogen (POC and PON) as well as Chlorophyll *a* (Chl*a*) were performed about 4 h after the start of the daily photoperiod. POC and PON samples were filtered onto precombusted (12 h, 500°C) glass fiber filters (GF/F, 0.7 µm nominal pore size; Whatman, Maidstone, UK). After drying for at least 24 h, filters were submitted to elemental analysis (EA 3000; EuroVector, Pavia, Italy) using the flash combustion technique (Knap *et al.*, 1996). Chl*a* samples were filtered onto precombusted (12 h, 500°C) glass fiber filters (GF/F 0.7 µm; Whatman), shock frozen in liquid nitrogen and stored at −80°C until extraction. Filters were extracted overnight in 5 ml acetone (90%, Sigma-Aldrich) after cell disruption in a cell-mill (Precellys 24, Bertin, Montigny-le-Bretonneux, France). Extracts were centrifuged (13 000 rcf for 5 min, 4K10; Sigma) and Chl*a* concentration in the supernatant was determined using the fluorometric 'acidification method' (TD-700 Fluorometer; Turner Designs, San Jose, CA, USA; Knap *et al.*, 1996).

Physiological assays

Gas fluxes of O_2 and CO_2 were measured at least 4 h after the start of the daily photoperiod using membrane-inlet mass spectrometry (MIMS; Isoprime; GV Instruments, Manchester, UK), following calibration procedures described in Rokitta & Rost (2012). Prior to the assays, cells were concentrated by gentle

filtration over polycarbonate filters (Isopore TSTP, 3 µm; Merck, Darmstadt, Germany) and resuspended in culture medium buffered to a pH_{NBS} of 8.0 (50 mM 4-(2-hydroxyethyl)-1-piperazineethanesulfonic acid; HEPES). Subsequently, cells were transferred into the temperature- and light-controlled MIMS cuvette. Carbonic anhydrase (500 µg l^{-1} final concentration) was added to ensure instantaneous equilibration of the carbonate system, and therefore, reported CO_2 fluxes comprise CO_2 as well as HCO_3^-. Photosynthesis-vs-irradiance (PI-) assays were performed in consecutive light–dark phases of *c.* 6 min each with increasing light intensities (50, 150, 250, 400 µmol photons m^{-2} s^{-1}). PI-assays were performed first under the acclimation temperatures (6°C or 15°C, respectively). Subsequently, the cuvette temperature was shifted to 15°C or 6°C, respectively, and the PI-assays were repeated to assess the abrupt effects of warming or cooling on the physiological processes.

Net rates of photosynthetic oxygen release and carbon uptake were obtained from O_2 and CO_2 fluxes during the light phases, while rates of respiratory oxygen uptake (R_{O_2}) and carbon release (R_{CO_2}) were obtained from O_2 and CO_2 fluxes during the dark phases. Gross rates of photosynthetic oxygen release (PS_{O_2}) and carbon uptake (PS_{CO_2}) were calculated by subtracting mean respiratory rates from net rates during light. Maximum photosynthetic rates (V_{max}), the light-use efficiencies (α), and the light saturation indices (I_k) were estimated by fitting the PI-curves to the model of Rokitta & Rost (2012). After the assays, Chl*a* samples were collected from the cuvette in duplicates and analysed as described above, to express the obtained rates based on Chl*a*. Assay data were based on 3–5 replicates, as in some cases physiological activity was too low to derive process rates.

Q_{10} factors were calculated, comparing physiological rates before and after the abrupt temperature shifts according to the formula $Q_{10} = \Delta k^{10°C/\Delta T}$ whereby k refers to the corresponding physiological rate. Photosynthetic (PQ) and respiratory quotients (RQ) were calculated from gross rates as $PQ = PS_{O_2}/PS_{CO_2}$ and $RQ = R_{CO_2}/R_{O_2}$.

Statistics

Results of acclimation responses were obtained as means with standard deviations of four biological replicates ($n = 4$) and confirmed to be normally distributed (Kolmorogov-Smirnov test). Acclimation responses were tested for significance using an unpaired two-sided Student's *t*-test. Results of physiological responses were obtained as means with standard deviation of three or more biological replicates ($n \geq 3$) and were likewise confirmed to be normally distributed. Increases or decreases in physiological rates in response to abrupt temperature shifts were tested for significance with a paired one-sided Student's *t*-test. To test for significant differences between acclimation temperatures, an unpaired two-sided Student's *t*-test was used. Q_{10} values were tested for significant differences by a one-way analysis of variances and additional post hoc test (Tukey). Differences in V_{max} rates after abrupt temperature increases were tested for significance using an unpaired one-sided Student's *t*-test. Differences in PQs and RQs in response to the abrupt temperature shifts were tested for significance using a paired two-sided Student's *t*-test, and for significant differences between acclimation temperatures by an unpaired two-sided Student's *t*-test. All statistics were performed using the statistics program JASP (Love *et al.*, 2019). The significance level was set to *, $P \leq 0.05$; **, $P \leq 0.01$; ***, $P \leq 0.001$.

Results

Acclimation responses

Growth rates of *P. tricornutum* increased significantly by 125% from 0.4 ± 0.01 d^{-1} at 6°C acclimation temperature to 0.9 ± 0.1 d^{-1} at 15°C acclimation temperature ($P < 0.05$; Fig. 1a). POC production rates increased significantly by 180% from 7.0 ± 0.3 pg $cell^{-1}$ d^{-1} at 6°C to 21 ± 4 at 15°C (Fig. 1b). POC quota increased significantly by 35% from 16.9 ± 0.9 pg $cell^{-1}$ at 6°C to 23.2 ± 3.4 pg $cell^{-1}$ at 15°C (Fig. 1c), whereas PON quota increased significantly by 55% from 2.7 ± 0.2 pg $cell^{-1}$ at 6°C to 4.1 ± 0.2 pg $cell^{-1}$ at 15°C acclimation temperature (Fig. 1d). This resulted in an insignificant decrease of the POC : PON ratio by 20% from 5.4 ± 0.3 at 6°C and 4.8 ± 0.9 at 15°C. Chl*a* quota increased significantly by 180% from 0.13 ± 0.03 pg $cell^{-1}$ at 6°C to 0.37 ± 0.02 pg $cell^{-1}$ at 15°C (Fig. 1e). Chl*a* : POC ratios increased significantly by 105% from 0.008 ± 0.001 (pg pg^{-1}) at 6°C to 0.016 ± 0.002 (pg pg^{-1}) at 15°C (Fig. 1f).

Physiological responses

Under *in-situ* light intensity, *P. tricornutum* experienced a stimulation of PS_{O_2}, PS_{CO_2}, and R_{O_2} in response to the abrupt temperature rises (Fig. 2a,b) and, vice versa, an inhibition in response to the abrupt temperature drop (Fig. 2a,b). The degree of stimulation upon warming was similar for these three processes, with Q_{10} factors of *c.* 1.6 (Table 1). The degree of inhibition upon cooling was equally strong for PS_{CO_2} ($1/Q_{10}$ *c.* 1.6; Table 1), while PS_{O_2} and R_{O_2} responded much more prominently ($1/Q_{10}$ *c.* 2.1; Table 1). After acclimation to 6°C and 15°C, however, rates of PS_{O_2}, PS_{CO_2} and R_{O_2} were, despite the temperature difference of almost 10°C, surprisingly similar to pretreatment levels (PS_{O_2} *c.* 190 µmol O_2 (mg Chl*a*)$^{-1}$ h^{-1}, PS_{CO_2} *c.* 130 µmol CO_2 (mg Chl*a*)$^{-1}$ h^{-1} and R_{O_2} *c.* 40 µmol O_2 (mg Chl*a*)$^{-1}$ h^{-1}; Fig. 2a,b). As a result, also PQs remained stable (*c.* 1.6; Table 1), and only experienced a transient, insignificant decrease (PQ *c.* 1.0) after the abrupt temperature drop.

In contrast to the above-described changes in $V_{in\text{-}situ}$ of PS_{O_2}, PS_{CO_2} and R_{O_2}, all of which responded to warming or cooling as hypothesized, R_{CO_2} showed an opposite response (Fig. 2b): It *decreased* in response to the abrupt temperature rise (Q_{10} *c.* 0.7; Table 1) and *increased* in response to the abrupt temperature drop ($1/Q_{10}$ *c.* 0.6). Also, no compensational behavior after acclimation was observed in R_{CO_2}, that is, cells maintained rates on a higher level (*c.* 60 µmol CO_2 (mg Chl*a*)$^{-1}$ h^{-1}) at low temperature, and vice versa on a lower level (*c.* 40 µmol CO_2 (mg Chl*a*)$^{-1}$ h^{-1}) at high temperature (Fig. 2b). This contrasting

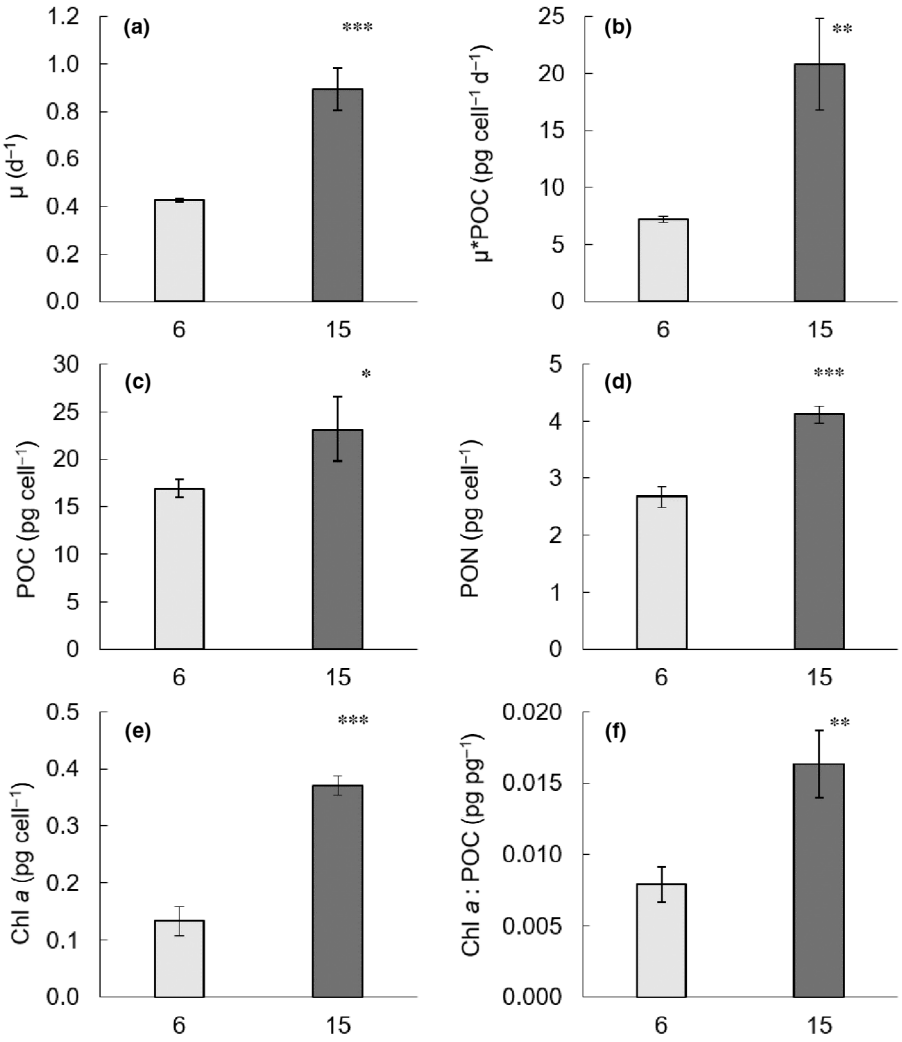

Fig. 1 Acclimation responses of *Phaeodactylum tricornutum* at 6°C (light grey) and 15°C (dark grey) acclimated cells. (a) Growth rates (μ); (b) production rates (μ×POC); (c) particulate organic carbon (POC) quota; (d) particulate organic nitrogen (PON) quota; (e) chlorophyll *a* (Chl*a*) quota; (f) Chl*a* : POC ratios. Error bars denote standard deviation. Significance levels between treatments are indicated by: *, $P \leq 0.05$; **, $P \leq 0.01$; ***, $P \leq 0.001$.

behavior of R_{O_2} and R_{CO_2} in response to acclimation temperature led to significantly different RQs at 6°C (*c.* 2.0) and 15°C (*c.* 0.9), this divergence being even slightly stronger after the abrupt temperature changes (Table 1).

Interestingly, analog to observations of photosynthetic rates under *in-situ* light intensity ($V_{in\text{-}situ}$), light saturated rates (V_{max}) of PS_{O_2} and PS_{CO_2} remained on a similarly high level (Fig. 2c,d), irrespective of the acclimation temperature. However, when 6°C acclimated cells experienced the abrupt temperature rise to 15°C, the V_{max} rates of both, PS_{O_2} and PS_{CO_2}, were synergistically stimulated. Hence, the combined stimulation by light and temperature was significantly stronger than by high light or temperature rise alone. Cells exhibited fluxes of *c.* 400 μmol O_2 or C (mg Chl*a*)$^{-1}$ h^{-1} under the combination of abrupt exposure to high temperature and high light, this being an increase of 94% (PS_{O_2}; Fig. 2c) and 191% (PS_{CO_2}; Fig. 2d) in comparison to $V_{in\text{-}situ}$ rates (Fig. 2a,b). In turn, in 15°C acclimated cells, V_{max} decreased by the abrupt temperature drop to a similar level as observed under $V_{in\text{-}situ}$ (Fig. 2a,b), indicating that the thermally induced inhibition could not be compensated by higher irradiance.

Discussion

Higher temperatures accelerate cellular metabolism

All assessed growth parameters were clearly stimulated by the higher temperature, confirming that *P. tricornutum* (strain CCAP 1052/1A) performs better under 15°C than under 6°C (Fig. 1). Studies on other diatoms often found opposing responses for growth and elemental quota with warming, that is, high growth rates result in low elemental quota since faster cell division lowers the apparent biomass content per cell (Thompson *et al.*, 1992; Hoppe *et al.*, 2018; Wolf *et al.*, 2018).

In our study, both growth rate (+125%, Fig. 1a) and POC quota (+35%, Fig. 1c) were stimulated by higher acclimation temperature, which also resulted in massively stimulated POC production rates (+180%, Fig. 1b) as well as seemingly larger cells (Fig. S1; in line with Li & Young, 2023). Consequently, the primary factor affecting POC quota in *P. tricornutum* seemed not to be the cell division rate, but net carbon uptake. This observation also confirms the hypothesis that anabolic processes (i.e. CO_2 fixation) are affected by warming differently than catabolic

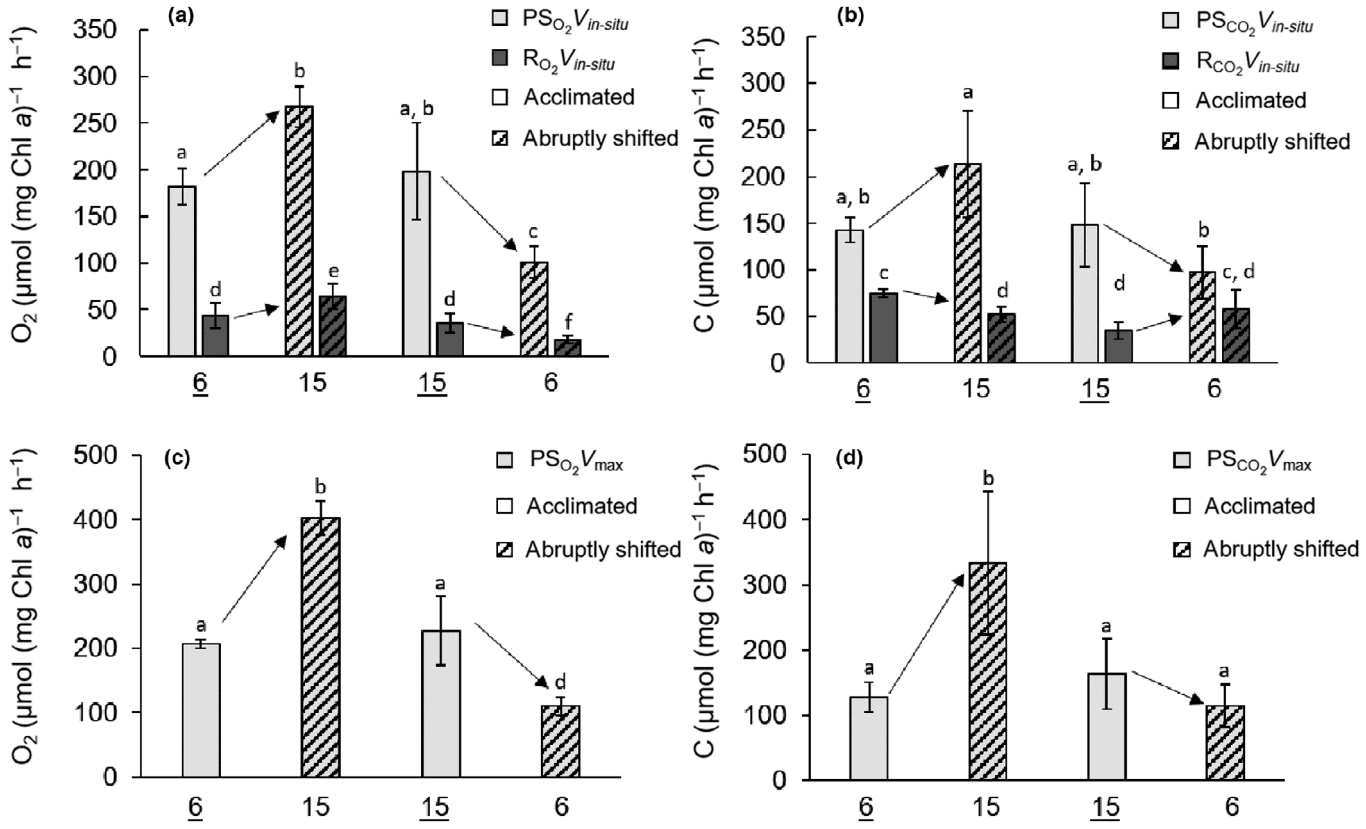

Fig. 2 Fluxes of O_2 and C in *Phaeodactylum tricornutum* corresponding to major physiological processes under acclimation temperature (light grey or dark grey filled; underlined temperature) and abruptly shifted temperature (hatched; not underlined). (a) gross rate of photosynthetic O_2 release (PS_{O_2} $V_{in\text{-}situ}$; light grey) and rate of respiratory O_2 uptake (R_{O_2}; dark grey) at *in-situ* light intensity; (b) gross rate of photosynthetic C uptake (PS_{CO_2} $V_{in\text{-}situ}$; light grey) and rate of respiratory C release (R_{CO_2}; dark grey) at *in-situ* light intensity; (c) gross rate of photosynthetic O_2 release under light saturation (PS_{O_2} V_{max}; light grey); (d) gross rate of photosynthetic C uptake under light saturation (PS_{CO_2} V_{max}; light grey). Arrows indicate assay direction. Letters indicate significance between treatments. Error bars denote standard deviation.

Table 1 Q_{10} factors of all measured physiological processes and PQs and RQs at *in-situ* light intensity of *Phaeodactylum tricornutum*.

Temp (°C)	6 → 15		15 → 6	
Q_{10} PS_{O_2}	1.5 ± 0.2^{a}		2.1 ± 0.6^{a}	
Q_{10} PS_{CO_2}	1.6 ± 0.5^{a}		$1.6 \pm 0.6^{a,b}$	
Q_{10} R_{O_2}	1.6 ± 0.2^{a}		2.2 ± 0.8^{a}	
Q_{10} R_{CO_2}	0.6 ± 0.1^{b}		0.7 ± 0.3^{b}	
PQ	1.6 ± 0.2^{a}	→ 1.6 ± 0.4^{a}	1.5 ± 0.3^{a}	→ 1.0 ± 0.4^{a}
RQ	2.0 ± 0.2^{a}	→ 0.8 ± 0.01^{b}	0.9 ± 0.3^{b}	→ 3.4 ± 1.1^{c}

PS_{O_2}, gross rate of photosynthetic O_2 release; PS_{CO_2}, gross rate of photosynthetic C uptake; R_{O_2}, rate of respiratory O_2 uptake; R_{CO_2}, rate of respiratory C release; PQ, photosynthetic quotient; RQ, respiratory quotient. Underlined temperatures indicate acclimation temperature, non-underlined temperatures indicate abrupt shifts. Q_{10} factors of the 15°C → 6°C assay are expressed as $1/Q_{10}$. Arrows indicate assay directions. Letters indicate significance between treatments. Values are expressed as means ± SD.

processes (i.e. respiratory CO_2 release), otherwise the phenotype would not have changed so remarkably.

Moreover, PON quota were even more strongly increased at 15°C (+55%, Fig. 1d) than POC quota, resulting in insignificantly decreased POC : PON ratios by 22%. Hence, cells apparently assimilated relatively more nitrogen relative to carbon, which in turn hints toward increased content of protein and light harvesting complexes. In line with this, Chl*a* quota increased more strongly under higher temperature (+180%, Fig. 1e) than POC quota, so that Chl*a* : POC ratios increased significantly (+105%, Fig.1f). Hence, the stimulation in Chl*a* quota at higher temperature is thus not a result of generally increased biomass, but indeed reflects the upregulation of photosynthetic machinery. These results are in line with previous reports on the dependency of Chl*a* on temperature in marine phytoplankton (Geider, 1987; Thompson *et al.*, 1992). Apparently, with increasing temperatures, light becomes 'more limiting', likely because high temperatures allow faster electron transfer reactions and diffusion of respective carrier molecules through membranes. Consequently, also processes downstream of the light reactions, that is the Calvin cycle and nitrate reduction, are accelerated and drain more electrons, which necessitates an increase of the light harvesting capacity (Raven & Geider, 1988; Thompson *et al.*, 1992). Thus, cells upregulate the abundance of light harvesting pigments in order to prevent a temperature-induced 'imbalance' in photosynthesis.

Abrupt over- and undershoots in physiological rates are synchronous and transient

In response to the abrupt temperature changes, rates of PS_{O_2}, PS_{CO_2}, and R_{O_2} were strongly stimulated or inhibited, respectively (Fig. 2a,b). This indicates that, as hypothesized, these processes are in the first instance controlled by the thermodynamics of the underlying physical and chemical phenomena, rather than by the enzymatic inventory, which does not change on these timescales. The stimulations of these processes were surprisingly similar (Q_{10} of 1.6, i.e. 50%; Table 1), resulting in a physiological balance. This was also reflected by the stable PQs of 1.4 (Table 1), which are in line with previously reported PQs of new production in microalgae (Eppley & Peterson, 1979; Laws, 1991). Interestingly, the abrupt temperature stimulation in PS_{O_2} and PS_{CO_2} was stronger under light saturation (i.e. V_{max}; Fig. 2c,d) than under *in-situ* irradiance (Fig. 2a,b). Apparently, enhanced membrane fluidity and electron transport after abrupt temperature rises enabled cells to exploit comparably high-light intensities and transiently maximize photosynthetic electron throughput. This benefit, however, was neither apparent under high-light exposure at acclimation temperatures nor was the adverse effect of abrupt cooling compensated by high light. Hence, *P. tricornutum* shifts from light saturation at low temperature to light limitation at high temperature. In line with this, I_k was increased in response to the abrupt temperature rise, but returned to its initial values over the course of acclimation (Table S2). In other words, I_k is temperature-dependent (Behrenfeld *et al.*, 2004) only on short timescales.

The inhibition after the abrupt temperature drop was of equal magnitude in PS_{O_2} and R_{O_2} ($1/Q_{10}$ of 2.0; Table 1), but it was less pronounced in PS_{CO_2} ($1/Q_{10}$ of 1.6; Table 1). This resulted in a transient imbalance between PS_{O_2} and PS_{CO_2} as evidenced by the PQ decreasing to 1.0 (Table 1). This less pronounced inhibition of PS_{CO_2} might originate from the fact that it is purely dependent on enzymatic reactions (Taiz & Zeiger, 2006). By contrast, PS_{O_2} and R_{O_2} rely to a large extent on the biochemical rate of involved electron transport chains, which are strongly controlled by membrane fluidity (Maksimov *et al.*, 2017), and are therefore highly temperature-dependent, more strongly than enzymatic processes (Los *et al.*, 2013). Also, the less pronounced inhibition of PS_{CO_2} may be explained by the increased carboxylation affinity of RubisCO with declining temperatures (Hall & Keys, 1983; Rokitta *et al.*, 2022), and the concomitantly increased $CO_2:O_2$ ratio in colder seawater (Jordan & Ogren, 1981; Zeebe & Wolf-Gladrow, 2001), which may further compensate the thermodynamic decrease of enzyme-catalyzed reaction rates.

Acclimation readjusts metabolism to a homeostatic 'sweet spot'

Even though cells experienced transient over- or undershoots when confronted with a substantially higher or lower temperature, the physiological machinery was adjusted over the course of acclimation, yielding notably different 'phenotypes', as evidenced by the measured acclimation parameters μ, POC, PON, and Chl*a* (Fig. 1). Interestingly, however, the Chl*a*-normalized rates of PS_{O_2}, PS_{CO_2} and R_{O_2} reverted to the very same, seemingly 'fixed' levels, that is *c.* 200 μmol O_2 (mg Chl*a*)$^{-1}$ h^{-1}, *c.* 125 μmol C (mg Chl*a*)$^{-1}$ h^{-1} and *c.* 50 μmol O_2 (mg Chl*a*)$^{-1}$ h^{-1}, respectively (Fig. 2a,b). Specifically, the tendency of cells to downscale their photosynthetic machinery under high temperature was surprising, as it causes a reversion to lower physiological rates than are obviously possible. It suggests that achieving highest-possible rates in single physiological processes is by no means an optimal strategy. Instead, cellular metabolism involves a compromise between biomass production, pigment use efficiency and the ability to respond flexibly to environmental changes, while minimizing 'material efforts' and stress due to unbalanced physiological processes (Behrenfeld *et al.*, 2008; Halsey & Jones, 2015).

As a consequence of the phenotypic changes, for example increased Chl*a* quota, the *cell-normalized* rates showed temperature-related changes that persisted even after acclimation (Table S3). Based on this comparison of Chl*a*- vs cell-normalized rates (Fig. 3), it becomes clear that the unaltered *quality* of the physiological apparatus, that is the sweet spot adjustment 'per-Chl*a*', ensures metabolic balance along the temperature gradient, whereas the *quantitative* changes along the temperature gradient alter the overall physiological output 'per-cell'. In other words, measuring physiological rates per Chl*a* in different temperature regimes does not give an idea of the potential of phytoplankton biomass growth and CO_2 removal. These ecological and also biogeochemical consequences of temperature changes can only be judged when normalizing rates to the standing stock biomass.

Plastidary reductant export throttles the TCA cycle under high temperature

In contrast to photosynthetic processes and the respiratory chain, the tricarboxylic acid cycle responded remarkably differently to the applied temperature changes: R_{CO_2} was significantly *decreased* at *higher* temperature and, in turn, remarkably *increased* under *lower* temperature, and no 'sweet spot behavior' was apparent (Fig. 2b). The opposing temperature response of the mitochondrial R_{O_2} and R_{CO_2} consequently resulted in a major physiological imbalance, also evidenced by high RQs at low temperature (i.e. >2, Table 1) and low RQs at high temperature (<1, Table 1). This indicates a persistent over- or under provision of the reductant carrier NADH under low or high temperatures, respectively. Nevertheless, R_{O_2} was maintained on a comparably high level even under acclimation. Also, growth rates and cellular quota of POC and PON indicated generally higher metabolic rates at 15°C. Consequently, under high temperature, there need to be sources of reductant to fuel the respiratory chain other than the TCA cycle.

R_{O_2} being prominently stimulated by high temperature has been observed before in *P. tricornutum* and other phytoplankton (Padfield *et al.*, 2016; Barton *et al.*, 2020). However, these authors assume that this stimulation likewise occurs in R_{CO_2}, which contradicts our observations. Our findings of increased

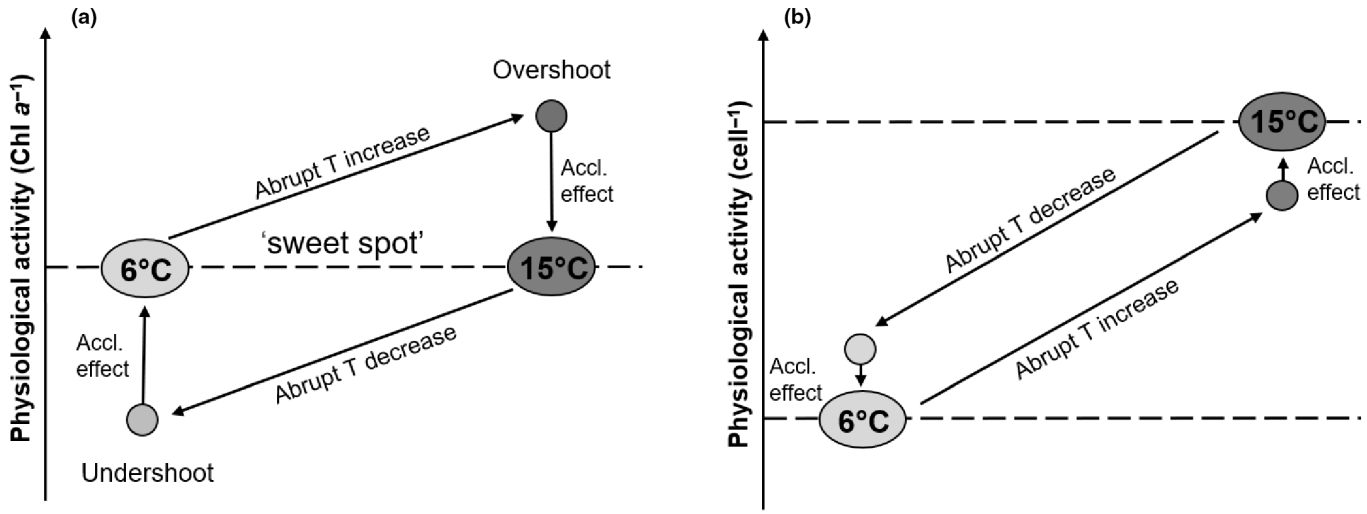

Fig. 3 Schematic temperature (T) responses of photosynthetic O_2 release, photosynthetic C uptake and respiratory O_2 uptake, (a) normalized to Chlorophyll *a* (Chla) and (b) to cells in *Phaeodactylum tricornutum* at 6°C (light grey) and 15°C (dark grey). Large ovals indicate physiological activity at acclimation temperature, small circles indicate physiological activity after abruptly shifted temperatures.

R_{O_2} and decreased R_{CO_2} under 15°C, based on gas flux measurements of the involved processes, are in line with the previously reported plastidial-mitochondrial reductant exchange in *P. tricornutum* (Bailleul *et al.*, 2015). This reductant exchange likely functions as alternative electron sink, since *P. tricornutum* lacks cyclic electron flow to increase the otherwise insufficient plastidial ATP : NADPH ratio (Curien *et al.*, 2016). This is especially necessary under elevated temperatures, since CO_2-concentrating mechanisms (CCM), which exploits the thylakoidal proton motive force (PMF) to import HCO_3^- from the alkaline stroma into the acidic lumen, are more active than at lower temperatures (Li & Young, 2023). As a consequence of the H^+-dependent conversion of HCO_3^- into CO_2 in the lumen, the PMF is partially consumed, thereby decreasing the plastidial ATP : NADPH ratio, or rather PMF : electron-transport ratio. In response to this apparent relative 'overreduction', reduction equivalents are exported and directed toward alternative sinks, in this case the mitochondrial oxidative phosphorylation, likely via malate shuttles (Kinoshita *et al.*, 2011; Prihoda *et al.*, 2012). Hence, R_{O_2} is partly fueled by the imported reduction equivalents from the chloroplast, thus the mitochondrial redox state shifts and R_{CO_2} is downregulated. At low temperature, the CCM is less active, consuming less PMF, and thereby lowering the need to export reduction equivalents. Consequently, at low temperature, mitochondrial oxidative phosphorylation is primarily fueled by the TCA cycle, evidenced by high R_{CO_2}. This phenomenon of alternative reductant sinks to avoid plastidial redox stress is also commonly known in other photosynthetic organisms. Land plants, for example, are assumed to reroute *c.* 10% of their total PSI driven electron flow into mitochondria (Noguchi & Yoshida, 2008). Typically, alternative electron flow is known to protect cells from photodamage under low temperature while cells are exposed to high-light intensities. However, such mechanisms as protection against high temperature induced redox stress are known in cow peas (*Vigna unguiculate*), which use cyclic electron flow to compensate for a higher temperature stimulation in photosynthetic light reaction than in C-fixation (Osei-Bonsu *et al.*, 2021). In our study, the plastidial-mitochondrial reductant exchange not only explains the opposing temperature response of R_{CO_2} and the persistently high R_{O_2} at 15°C, but also the much higher biomass retention and thus, the phenotypic change in POC quotas under higher temperature.

Conclusion

This study resolves the mechanistical effects of temperature on physiological sub-processes in *P. tricornutum* under suboptimal and close-to-optimal temperatures. Cells experienced a clear stimulation in growth, biomass production and pigmentation under higher temperature, mainly driven by the downregulation of the respiratory CO_2 loss. This downregulation is caused by a plastid-to-mitochondrial reductant export that in a wider sense serves to also increase the photosynthetic ATP : NADPH ratio. Interestingly, the other investigated physiological sub-processes experienced transient and synchronous over- or undershoots in response to abrupt warming or cooling, and were re-adjusted to homeostatic 'sweet-spot' levels in the course of acclimation. Our data further show that abrupt temperature increases enable cells to transiently exploit very high-light intensities, suggesting that processes involving electron transfer chains (photosynthetic light reactions, respiratory O_2 consumption) are more prone to temperature effects than, for example, enzymatic processes. Future studies should expand this experimental approach in order to elucidate the physiological bottlenecks and organelle crosstalk when temperatures become supra-optimal, that is, detrimental.

Acknowledgements

We thank Klaus-Uwe Richter for technical support with MIMS measurements. We also thank Tina Brenneis, Marcel Machnik

and Laura Wischnewski for their support in measurements of carbonate chemistry, Chlorophyll *a* as well as POC and PON. Additionally, we want to thank Prof. Dr Kai Bischof for helpful discussions. Funding was provided by Alfred-Wegener-Institute Bremerhaven, Helmholtz-Centre for Polar and Marine Research. Open Access funding enabled and organized by Projekt DEAL.

Competing interests

None declared.

Author contributions

LR, BR and SR designed the study and discussed data interpretation. LR performed the experiments. LR and SR analyzed the data. LR wrote the manuscript with input of BR and SR.

ORCID

Linda Rehder https://orcid.org/0000-0002-2835-7242
Sebastian D. Rokitta https://orcid.org/0000-0002-7540-9033
Björn Rost https://orcid.org/0000-0001-5452-5505

Data availability

The data that support the findings of this study are available in the Supporting Informtion of this article.

References

Angilletta MJ Jr, Angilletta MJ. 2009. *Thermal adaptation: a theoretical and empirical synthesis*. Oxford, UK: Oxford University Press.

Bailleul B, Berne N, Murik O, Petroutsos D, Prihoda J, Tanaka A, Villanova V, Bligny R, Flori S, Falconet D. 2015. Energetic coupling between plastids and mitochondria drives CO_2 assimilation in diatoms. *Nature* **524**: 366–369.

Barton S, Jenkins J, Buckling A, Schaum C-E, Smirnoff N, Raven JA, Yvon-Durocher G. 2020. Evolutionary temperature compensation of carbon fixation in marine phytoplankton. *Ecology Letters* **23**: 722–733.

Beardall J, Raven JA. 2004. The potential effects of global climate change on microalgal photosynthesis, growth and ecology. *Phycologia* **43**: 26–40.

Behrenfeld MJ, Halsey KH, Milligan AJ. 2008. Evolved physiological responses of phytoplankton to their integrated growth environment. *Philosophical Transactions of the Royal Society B: Biological Sciences* **363**: 2687–2703.

Behrenfeld MJ, Prasil O, Babin M, Bruyant F. 2004. In search of a physiological basis for covariations in light-limited and light-saturated photosynthesis 1. *Journal of Phycology* **40**: 4–25.

Bissinger JE, Montagnes DJS, Sharples J, Atkinson D. 2008. Predicting marine phytoplankton maximum growth rates from temperature: improving on the Eppley curve using quantile regression. *Limnology and Oceanography* **53**: 487–493.

Boyd PW, Rynearson TA, Armstrong EA, Fu F, Hayashi K, Hu Z, Hutchins DA, Kudela RM, Litchman E, Mulholland MR. 2013. Marine phytoplankton temperature versus growth responses from polar to tropical waters–outcome of a scientific community-wide study. *PLoS ONE* **8**: e63091.

Brown JH, Gillooly JF, Allen AP, Savage VM, West GB. 2004. Toward a metabolic theory of ecology. *Ecology* **85**: 1771–1789.

Cooley S, Schoeman D, Bopp L, Boyd P, Donner S, Ghebrehiwet DY, Ito S-I, Kiessling W, Martinetto P, Ojea E *et al.* 2022. Oceans and coastal ecosystems and their services. In: Pörtner H-O, Roberts DC, Tignor M, Poloczanska ES, Mintenbeck K, Alegría A, Craig M, Langsdorf S, Löschke S, Möller V *et al.*, eds. *Climate change 2022: impacts, adaptation and vulnerability*. Contribution of Working Group II to the Sixth Assessment Report of the Intergovernmental Panel on Climate Change. Cambridge, UK: Cambridge University Press, 379–550.

Curien G, Flori S, Villanova V, Magneschi L, Giustini C, Forti G, Matringe M, Petroutsos D, Kuntz M, Finazzi G. 2016. The water to water cycles in microalgae. *Plant and Cell Physiology* **57**: 1354–1363.

Doney SC, Ruckelshaus M, Emmett Duffy J, Barry JP, Chan F, English CA, Galindo HM, Grebmeier JM, Hollowed AB, Knowlton N. 2012. Climate change impacts on marine ecosystems. *Annual Review of Marine Science* **4**: 11–37.

Eppley RW. 1972. Temperature and phytoplankton growth in the sea. *Fishery Bulletin* **70**: 1063–1085.

Eppley RW, Peterson BJ. 1979. Particulate organic matter flux and planktonic new production in the deep ocean. *Nature* **282**: 677–680.

Falkowski P, Scholes RJ, Boyle E, Canadell J, Canfield D, Elser J, Gruber N, Hibbard K, Högberg P, Linder S *et al.* 2000. The global carbon cycle: a test of our knowledge of earth as a system. *Science* **290**: 291–296.

Falkowski PG, Barber RT, Smetacek V. 1998. Biogeochemical controls and feedbacks on ocean primary production. *Science* **281**: 200–206.

Falkowski PG, Raven JA. 2013. *Aquatic photosynthesis*. Princeton, NJ, USA: Princeton University Press.

Field CB, Behrenfeld MJ, Randerson JT, Falkowski P. 1998. Primary production of the biosphere: integrating terrestrial and oceanic components. *Science* **281**: 237–240.

Finkel ZV, Beardall J, Flynn KJ, Quigg A, Rees TAV, Raven JA. 2009. Phytoplankton in a changing world: cell size and elemental stoichiometry. *Journal of Plankton Research* **32**: 119–137.

Gao K, Campbell DA. 2014. Photophysiological responses of marine diatoms to elevated CO_2 and decreased pH: a review. *Functional Plant Biology* **41**: 449–459.

Geider RJ. 1987. Light and temperature dependence of the carbon to chlorophyll *a* ratio in microalgae and cyanobacteria: implications for physiology and growth of phytoplankton. *New Phytologist* **106**: 1–34.

Guillard RR, Ryther JH. 1962. Studies of marine planktonic diatoms: I. *Cyclotella nana* Hustedt, and *Detonula confervacea* (Cleve) Gran. *Canadian Journal of Microbiology* **8**: 229–239.

Hall NP, Keys AJ. 1983. Temperature dependence of the enzymic carboxylation and oxygenation of ribulose 1,5-bisphosphate in relation to effects of temperature on photosynthesis. *Plant Physiology* **72**: 945–948.

Halsey KH, Jones BM. 2015. Phytoplankton strategies for photosynthetic energy allocation. *Annual Review of Marine Science* **7**: 265–297.

Hancke K, Glud RN. 2004. Temperature effects on respiration and photosynthesis in three diatom-dominated benthic communities. *Aquatic Microbial Ecology* **37**: 265–281.

Hegarty T. 1973. Temperature coefficient (Q_{10}), seed germination and other biological processes. *Nature* **243**: 305–306.

Hobday AJ, Alexander LV, Perkins SE, Smale DA, Straub SC, Oliver EC, Benthuysen JA, Burrows MT, Donat MG, Feng M. 2016. A hierarchical approach to defining marine heatwaves. *Progress in Oceanography* **141**: 227–238.

Hoppe CJM, Flintrop CM, Rost B. 2018. The Arctic picoeukaryote *Micromonas pusilla* benefits synergistically from warming and ocean acidification. *Biogeosciences* **15**: 4353–4365.

Hoppe H-G, Gocke K, Koppe R, Begler C. 2002. Bacterial growth and primary production along a north–south transect of the Atlantic Ocean. *Nature* **416**: 168–171.

Jordan DB, Ogren WL. 1981. Species variation in the specificity of ribulose biphosphate carboxylase/oxygenase. *Nature* **291**: 513–515.

Kinoshita H, Nagasaki J, Yoshikawa N, Yamamoto A, Takito S, Kawasaki M, Sugiyama T, Miyake H, Weber AP, Taniguchi M. 2011. The chloroplastic 2-oxoglutarate/malate transporter has dual function as the malate valve and in carbon/nitrogen metabolism. *The Plant Journal* **65**: 15–26.

Knap A, Michaels A, Close A, Ducklow H, Dickson A. 1996. Protocols for the joint global ocean flux study (JGOFS) core measurements. *JGOFS, Reprint of the IOC Manuals and Guides No. 29, UNESCO 1994*.

Laws EA. 1991. Photosynthetic quotients, new production and net community production in the open ocean. *Deep Sea Research Part A. Oceanographic Research Papers* **38**: 143–167.

Li M, Young JN. 2023. Temperature sensitivity of carbon concentrating mechanisms in the diatom *Phaeodactylum tricornutum*. *Photosynthesis Research* **156**: 1–11.

Los DA, Mironov KS, Allakhverdiev SI. 2013. Regulatory role of membrane fluidity in gene expression and physiological functions. *Photosynthesis Research* **116**: 489–509.

Love J, Selker R, Marsman M, Jamil T, Dropmann D, Verhagen J, Ly A, Gronau QF, Šmíra M, Epskamp S *et al.* 2019. JASP: graphical statistical software for common statistical designs. *Journal of Statistical Software* **88**: 1–17.

Maksimov EG, Mironov KS, Trofimova MS, Nechaeva NL, Todorenko DA, Klementiev KE, Tsoraev GV, Tyutyaev EV, Zorina AA, Feduraev PV. 2017. Membrane fluidity controls redox-regulated cold stress responses in cyanobacteria. *Photosynthesis Research* **133**: 215–223.

Meehl GA, Tebaldi C. 2004. More intense, more frequent, and longer lasting heat waves in the 21st century. *Science* **305**: 994–997.

Nelson DM, Tréguer P, Brzezinski MA, Leynaert A, Quéguiner B. 1995. Production and dissolution of biogenic silica in the ocean: revised global estimates, comparison with regional data and relationship to biogenic sedimentation. *Global Biogeochemical Cycles* **9**: 359–372.

Noguchi K, Yoshida K. 2008. Interaction between photosynthesis and respiration in illuminated leaves. *Mitochondrion* **8**: 87–99.

Osei-Bonsu I, McClain AM, Walker BJ, Sharkey TD, Kramer DM. 2021. The roles of photorespiration and alternative electron acceptors in the responses of photosynthesis to elevated temperatures in cowpea. *Plant, Cell & Environment* **44**: 2290–2307.

Padfield D, Yvon-Durocher G, Buckling A, Jennings S, Yvon-Durocher G. 2016. Rapid evolution of metabolic traits explains thermal adaptation in phytoplankton. *Ecology Letters* **19**: 133–142.

Pearle P, Collett B, Bart K, Bilderback D, Newman D, Samuels S. 2010. What Brown saw and you can too. *American Journal of Physics* **78**: 1278–1289.

Pörtner HO, Bennett AF, Bozinovic F, Clarke A, Lardies MA, Lucassen M, Pelster B, Schiemer F, Stillman JH. 2006. Trade-offs in thermal adaptation: the need for a molecular to ecological integration. *Physiological and Biochemical Zoology* **79**: 295–313.

Prihoda J, Tanaka A, de Paula WB, Allen JF, Tirichine L, Bowler C. 2012. Chloroplast-mitochondria cross-talk in diatoms. *Journal of Experimental Botany* **63**: 1543–1557.

Raven JA, Beardall J. 2022. Evolution of phytoplankton in relation to their physiological traits. *Journal of Marine Science and Engineering* **10**: 194.

Raven JA, Geider RJ. 1988. Temperature and algal growth. *New Phytologist* **110**: 441–461.

Riebesell U, Schulz KG, Bellerby RGJ, Botros M, Fritsche P, Meyerhöfer M, Neill C, Nondal G, Oschlies A, Wohlers J *et al.* 2007. Enhanced biological carbon consumption in a high CO_2 ocean. *Nature* **450**: 545–548.

Rokitta SD, Kranz SA, Rost B. 2022. Inorganic carbon acquisition by aquatic primary producers. In: *Blue planet, red and green photosynthesis: productivity and carbon cycling in aquatic ecosystems*. London, UK: ISTE-Wiley, 81–132.

Rokitta SD, Rost B. 2012. Effects of CO_2 and their modulation by light in the life-cycle stages of the coccolithophore *Emiliania huxleyi*. *Limnology and Oceanography* **57**: 607–618.

Rousseau V. 2000. *Dynamics of Phaeocystis and diatom blooms in the eutrophicated coastal waters of the Southern Bight of the North Sea*. PhD thesis, Universite Libre de Bruxelles, Brussels, Belgium.

Sabir JS, Theriot EC, Manning SR, Al-Malki AL, Khiyami MA, Al-Ghamdi AK, Sabir MJ, Romanovicz DK, Hajrah NH, El Omri A. 2018. Phylogenetic analysis and a review of the history of the accidental phytoplankter, *Phaeodactylum tricornutum* Bohlin (Bacillariophyta). *PLoS ONE* **13**: e0196744.

Schuback N, Hoppe CJ, Tremblay JÉ, Maldonado MT, Tortell PD. 2017. Primary productivity and the coupling of photosynthetic electron transport and carbon fixation in the Arctic Ocean. *Limnology and Oceanography* **62**: 898–921.

Taiz L, Zeiger E. 2006. *Fisiologia vegetal*. Castelló de la plana, Spain: Universitat Jaume I.

Thompson PA, Mx G, Harrison PJ, Whyte JN. 1992. Effects of variation in temperature. II. On the fatty acid composition of eight species of marine phytoplankton 1. *Journal of Phycology* **28**: 488–497.

Tréguer P, Nelson DM, Van Bennekom AJ, DeMaster DJ, Leynaert A, Quéguiner B. 1995. The silica balance in the world ocean: a reestimate. *Science* **268**: 375–379.

Wolf KK, Hoppe CJ, Rost B. 2018. Resilience by diversity: large intraspecific differences in climate change responses of an Arctic diatom. *Limnology and Oceanography* **63**: 397–411.

Zeebe RE, Wolf-Gladrow D. 2001. *CO_2 in seawater: equilibrium, kinetics, isotopes*. Houston, TX, USA: Gulf Professional Publishing.

Supporting Information

Additional Supporting Information may be found online in the Supporting Information section at the end of the article.

Fig. S1 Light microscopy of *Phaeodactylum tricornutum* at 6°C and 15°C acclimation temperature.

Table S1 Carbonate chemistry during acclimation in cultures of *Phaeodactylum tricornutum* at 6°C and 15°C acclimation temperature.

Table S2 Light saturation index and light use efficiency of gross photosynthetic O_2 release and gross photosynthetic C uptake normalized to Chlorophyll *a* in *Phaeodactylum tricornutum* at 6°C and 15°C acclimation temperatures as well as after the abrupt temperature shift.

Table S3 Physiological rates of gross photosynthetic O_2 release, gross photosynthetic C uptake, respiratory O_2 uptake, and respiratory C release in *Phaeodactylum tricornutum* normalized to cell density.

Please note: Wiley is not responsible for the content or functionality of any Supporting Information supplied by the authors. Any queries (other than missing material) should be directed to the *New Phytologist* Central Office.